

## Chapter

# Heat Recovery from Cryptocurrency Mining by Liquid Cooling Technology

*Nan Chen, Yunshui Chen and He Zhao*

## Abstract

Bitcoin, the world's largest cryptocurrency, currently consumes an estimated 150 terawatt-hours of electricity annually. Most cryptocurrency miners have dissipated the thermal energy from mining chips to the ambient by air cooling circulation. To recover the thermal energy from cryptocurrency mining, an advanced heat recovery system has been developed, prototyped, and tested. The cryptocurrency miners in an enclosure are cooled by spraying dielectric coolant, then the coolant heated by the mining chips is collected and driven through the spiral heating coil immersed in a 190 L hot water tank. High efficient liquid spray cooling mechanism is the core of this design, by which maximum coolant temperature can reach 70°C in the field trial within the safe temperature limits of mining chips. In practice, this record temperature not only meets the minimum legionellosis risk management requirements for building water systems defined by ANSI/ASHRAE Standard 188-2018 but also provides high-grade energy input to the building, district heating system, or booster heat pump/boiler if needed. In theory, the conventional concept of PUE based on energy has been redefined by the PUE based on exergy. The energy-based PUE is 1.03 and the exergy-based PUE is 0.95 in this case, which can truly reflect the useful energy flow, exergy, in the heat reclaim system.

**Keywords:** heat reclaim, cryptocurrency miner, exergy, liquid spray cooling, PUE

## 1. Introduction

Bitcoin, the world's largest cryptocurrency, currently consumes an estimated 150 terawatt-hours of electricity annually-more than the entire country of Argentina, with a population of 45 million [1]. Acknowledging that Bitcoin mining is a high energy consuming and high energy density industry, correspondingly, miners generated large quantities of heat during the continuous hashing process, which conventionally has been dissipated into the ambient by air cooling circulation. Regarding the financial and environmental benefits from the heat reuse in mining industry, competitive entities are explored an economical approach to elevate the revenue performance and cut the carbon footprint at initial stage of project plan and make effort to maximize these benefits further by advanced heat exchanging technologies, which can partially

or completely replace the traditional fossil fuels in the field of low temperature heating. Due to the resilience of spatial arrangement, miners can be deployed in the pattern of centralized and decentralized models. Centralized mining farms are more suitable to heat the green house, vertical farm, district heating network, i.e., work as a heat resource in a large scale. On the contrast, decentralized mining utilities can provide the space heating or hot water in the small-scale projects, such as in residential or light commercial deployment.

Heat recovery is a low-carbon technology that cuts across multiple sectors of the technologies. From the perspective of the first law of thermodynamics, the primary challenge is to identify effective ways to capture and transfer heat, along with sound economic use cases. From the perspective of the second law of thermodynamics, the second challenge is to elevate the grade of heat expelled by miners to extend the scope of waste heat application and provide feasibility to seamless connection with the current heat system driven by electricity or fossil fuels. Regarding the approaches of capture and transferring heat from miners, current technologies can be categorized into three types, i.e. air cooling, liquid immersion cooling (single phase and two phases), and hybrid (air/liquid) cooling [2]. Air cooling utilizes fans to pass air over the miner heat sinks. Hampus [3] reports that 5.5–30.5% of the electrical input to a 1 MW air-cooled mining farm could be recovered, which can fill the heating demand of a 2000m<sup>2</sup> greenhouse by 89.7–97.9%, and a 10,000 m<sup>2</sup> greenhouse by 50.0–61.5% respectively. Up to 94.5% of thermal energy has been wasted due to the poor thermal properties of air in the process of thermal transmission. Enachescu [4] pointed out that waste heat from a 45 MW data centre is sufficient to provide a year-round heating to a 8.34-acre greenhouse for commercial cannabis growth. The total annual avoided emissions were calculated at 70,000 tonnes of CO<sub>2</sub> by economizer cycles and waste heat reuse in Alberta, Canada. Agrodome [5] is the first retail facility that uses servers as heat sources distributing residual heat through a cascading set of greenhouse applications. Blockchain Dome, each dome has an input of 1.5 MW and produces 5,000,000 BTU/h of heated air, requires no additional electricity to maintain the preferred temperature range. In July of 2018, United American Corp. [6] announced their intention to deploy 25 Blockchain Domes across Quebec, filing a power license request at 5 MW at the large power preferential rate. Data center heat reuse co-location with an associated greenhouse minimizes losses to electricity distribution, heat transportation, and associated heat loss, which is a primary scenario for heat recovery from the air-cooled data center.

Immersion cooling is an IT cooling practice by which IT components and other electronics, including complete servers and storage devices, are submerged in a thermally conductive but electrically insulating dielectric liquid or coolant (single-phase or two-phase). Heat is removed from the system by circulating relatively cold liquid into direct contact with hot components, then circulating the now heated liquid through cool heat exchangers. The advantages of using liquid cooling over air cooling include liquid's higher specific heat capacity, density, and thermal conductivity. This allows liquid to transmit heat over greater distances with much less volumetric flow and reduced temperature difference. Regarding the higher coolant temperature, inlet water temperatures [7] in the order of 45–70°C can cool server rack chips and CPUs to approximately 80–90°C to avoid triggering the auto frequency throttling protection, while the maximum permissible temperature range of processors is 100–120°C. According to [8], the inlet temperatures can range between 30 and 60°C. The solution presented by Ernest Orlando Lawrence Berkeley National Laboratory [9] has an inlet temperature between 15 and 45°C, whereas the case study presented in [10] has an

inlet temperature of 50°C. Other advantages are the considerable fan energy saving and a lower noise level. The main drawback of liquid-cooled systems is the introduction of liquid within the data center and the potential damage that a failure can cause. In 2022, Bitcoin mining company Mint Green to deliver an innovative low-carbon mining waste solution to heat the City of North Vancouver, BC [11]. Production of both bitcoin and usable thermal energy positions the Digital Boilers to be the cost-leading low-carbon heating technology. In MintGreen design, the hash boards have been placed radially in a bell mouth-like chamber, submerged fully in the single-phase dielectric fluid. The cold coolant will flow in the chamber along the central line, be heated by the radial located hash boards, and then be collected circumferentially. Wisemining's digital boiler designed for residential mining and heating [12] includes a tank container design for ASIC and a 200-liter water tank with two heat exchangers. This product was designed based on two-phase immersion cooling concepts. The drawbacks of two-phase liquid are the coolant is expensive and highly leakable; The condensation of two-phase fluid in the inner tube driven by thermosiphon has a comparatively lower efficiency than that driven by forced convective heat transfer; The position of the miner must be lower than the coil in the water tank, which needs more footprint of this product.

Hybrid liquid-cooled systems are defined by the integration of the direct-to-chip liquid cooling of some high heat density components such as CPUs and DIMMs by microchannel flow [8, 13] or cold-plate heat exchangers [9, 14], with the air cooling of the rest of low heat density components. A 15 kW IBM rack as a typical example of a hybrid liquid cooled system has been tested [3, 15] under different ambient temperatures. This chiller-less rack can work under inlet coolant temperature of up to 45°C. In the summer season, its IT load of 13.16 kW can be maintained under 0.442 kW cooling power consumption. The average cooling power for a full year could be expected to be below 3.5%.

## 2. Objectives

Doubtless to say, the implementation of waste heat recovery measures in the crypto mining industry to building or district heating, absorption cooling, Rankine Cycle, Organic Rankine Cycle (ORC), biomass co-location, and desalination for clean water production, can tremendously improve financial performance and reduce CO<sub>2</sub> emissions. Nevertheless, the main impediment to introducing this technology in the data center is the low quality of the heat produced from electronic devices, despite the large quantity. The quality of heat is bound by the upper-temperature limits of electronics, which in most cases remain below 85°C. Air cooling is limited by the thermal properties of air which require co-located siting, making the retrofit into the existing data center impossible. The temperature difference across the inlet and outlet of the hybrid air portion is low due to the water loop removing most of the heat, thus the air cooler portion can operate at a low capacity and the water portion should be targeted for heat recovery. Two-phase immersion cooling is restricted by its characteristic of the saturated temperature-pressure curve which must be realized by a complicated evaporation-recondensation structure. As far as the grade/quality of the heat recovered by the above three approaches is concerned, air cooling typically results in outlet temperatures of 25 to 35°C, while outlet temperatures of up to 60°C are possible with single-phase immersion and hybrid liquid cooling [16]. The max. Temperature of two-phase immersion cooling relies on the selection of two-phase

coolant and max. Case temperature of chips. 3 M Novec 7100 with 61°C boiling point @ 1 atm is the most common working fluid in two-phase open bath immersion cooling. Even though Marcinichen [17] reports that high temperatures as 60–70°C for liquid-cooled systems and 70–80°C for two-phase cooling systems provide higher waste heat quality and open up a wide range of waste heat reuse opportunities. These temperatures were achieved in the complex direct on-chip evaporator by HFC134a or HFO1234ze under a working pressure of approx. 15 bar. Kuncoro [18] reports that the temperature differential between chips and coolant can be reduced up to 91.3% by the replacement of air cooling with single-phase oil cooling. It not only reveals the reason liquid cooling is a better option to harvest the high-grade thermal energy but also points out the direction to improve it continuously.

In this article, the prototype of a digital boiler has been designed and built that is helping reduce greenhouse gas emissions by repurposing the heat produced by their ASICs. The miner is cooled by spraying coolant, with intend to enhance heat transferring and consequently elevated coolant outlet temperature for high-grade heat recovery. The concept of PUE based on energy has been redefined accordingly regarding the exergy in the reclaimed heat, catering to the demands of reasonable performance evaluation of data center with thermal energy reuse. Experimental testing validated the exergy efficiency of this innovative design.

### **3. Design of digital boiler**

#### **3.1 Spray cooling mechanism-theory**

Why spray cooling has been selected as an alternative to extensively used immersion cooling and how to determine the parameters of spray cooling are the challenges in this design. Tracking the motion trajectory of the coolant liquid out of the sprayer, spreading out of the sprayer holes, receding due to viscous effects, splashing by droplet collision, stationary film generating by fluid viscosity on the solid surface, liquid film flowing by liquid momentum and gravity, and liquid flooding and draining will happen in sequence [19, 20]. The interfacial flow of coolant liquid film on the heat sink surface determines the flow pattern of film, through which heat transfer will happen. The flow patterns of droplets out of the sprayer depends basically on their outlet velocity, which are single droplet, droplet train, and droplet burst in the sequence of velocity increments. The impinging momentum of droplets onto the film attached to the solid surface coupled with the film flow pattern are the two main factors of the heat transfer mechanism of spray cooling. In this study, the droplet flow is designed as the droplet train flow- fresh droplets continuously impact the surface at a certain frequency. To investigate the heat transfer of spray cooling from this aspect, Soriano et al. [21] found that the decisive factor to achieve optimal cooling performance is to let the film velocity not be disturbed by the adjacent droplet streams. Zhang et al. [22, 23] further proved that both impact spacing and impingement pattern affect local and global cooling performance on the hot surface. The droplet train impingement among various impingement patterns is the best one for the highest thermal performance, which has also been recommended by Gao [24] after comparing the circular jet impingement cooling with droplet train impingement. As an advanced methodology [25], droplet trains broken by piezoelectric nozzles from more groups of jet flow can make cooling heat flux up to  $\sim 170 \text{ W/cm}^2$  with a nozzle diameter of 25  $\mu\text{m}$ .

In the field of Fluid Dynamics, Nusselt number ( $N_u$ ) is the ratio of convective to conductive heat transfer at a boundary in a fluid, by which the convective heat transfer coefficient could be calculated.

$$N_u = hL/k \quad (1)$$

where  $h$  is the convective heat transfer coefficient of the flow,  $L$  is the characteristic length,  $k$  is the thermal conductivity of the fluid.

In the single-phase regime, Rybicki and Mudawar [26] proposed the correlation for dielectric PF-5050 spray, which is

$$N_u = 4.7R_e^{0.61}P_r^{0.32} \quad (2)$$

in which  $R_e$  is Reynolds number and  $P_r$  is Prandtl number.

As the heat transferring mechanism of immersion cooling,  $N_u$  of an isothermal flat plate at a specified temperature in the free stream flow can be calculated by [27, 28]:

$$\text{For Laminar flow } (R_e < 5 \times 10^5) : N_u = 0.664R_e^{0.5}P_r^{0.33} \quad (3)$$

Refer to the quantitative comparison in **Figure 1** with constant  $P_r$  as 95 and  $R_e$  varying from 0 to 4500,  $N_u$  of spray flow from Eq. (2) is far higher than that of laminar flow in Eq. (3). Refer to Eq. (1), no doubt to say that  $h$  in spray flow will be much higher than that in immersion cooling. In this case, to get the optimal convection heat transfer coefficient coupled with minimal pressure drop and coolant distribution, a series of testing has been conducted to get the best diameter and distribution of spraying holes. 0.6 mm spraying hole has been proved to be a good option to achieve the droplet train flow and can wet the surface of the heat sink effectively.

**Figure 1** presents the comparison of  $N_u$  between single-phase spray and single-phase immersion under  $R_e$  number varying from 0 to 4500.  $N_u$  will be 200 for immersion cooling, and 3100 for spray cooling with  $R_e$  number 4000. It means under the same access liquid velocity, spray cooling can create much higher heat transferring coefficient than immersion cooling.

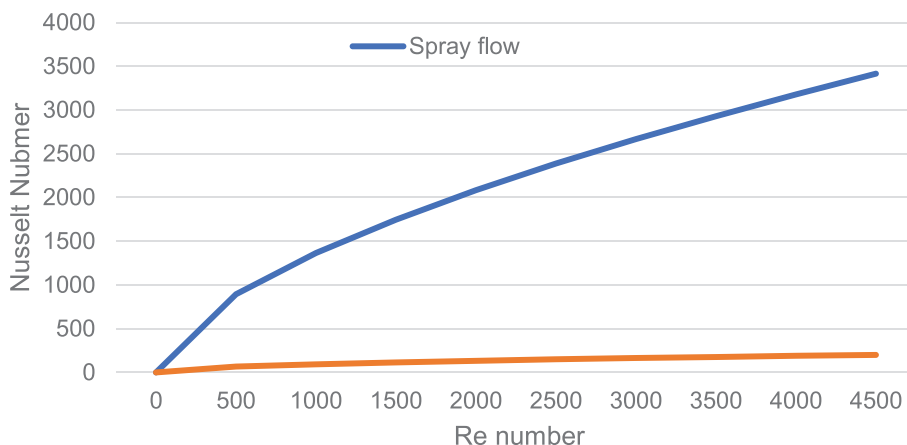


**Figure 1.** Comparison of  $N_u$  between single-phase spray and single-phase immersion under  $R_e$  number varying from 0 to 4500.

### 3.2 Spray cooling mechanism-design

**Figure 2** presents a schematic diagram of dielectric coolant being sprayed on the hash boards and heat sinks. The noisy fans in the air-cooled design have been removed and replaced by a liquid sprayer in the liquid cooling. The miner with the original heat sinks designed for air-cool was installed vertically in the reservoir, then the coolant was sprayed out of the sprayer from the top and access to hash boards and heat sinks. The coolant flush on the surface of the heat sink and drained automatically by gravity. The liquid film on the surface of the heat sink can be kept at its minimal thickness due to the excellent drainage and forceful flushing momentum. The surface area of the front and back heat sink indicates the different heat loads on the front and back side of the hash board, the spraying flow to them is distributed accordingly. The spraying holes on the top sprayer have been pinpointed to the heat sinks and their spatial distribution has been arranged based on the heat load distribution which can guarantee enough wetting on the surface of the heat sink for the best thermal performance with the least coolant consumption.

### 3.3 Digital boiler-design

In **Figure 3**, a modular heat recovery system by the name of Digital Boiler has been developed for hot water heating. This modular can be extended or combined to be an array providing higher heat capacity. This modular digital boiler includes four major kits, i.e. miner liquid cooling chassis, water tank kit, water replenishing kit, and dry cooler. The thermal energy generated from the miner including three hash boards (WhatsMiner M30S) will heat the dielectric coolant (7.3 L coolant charged) in the enclosure and then be suctioned into the pump (a DC permanent magnet pump). The heated dielectric coolant out of the pump will flow into the line connected with the

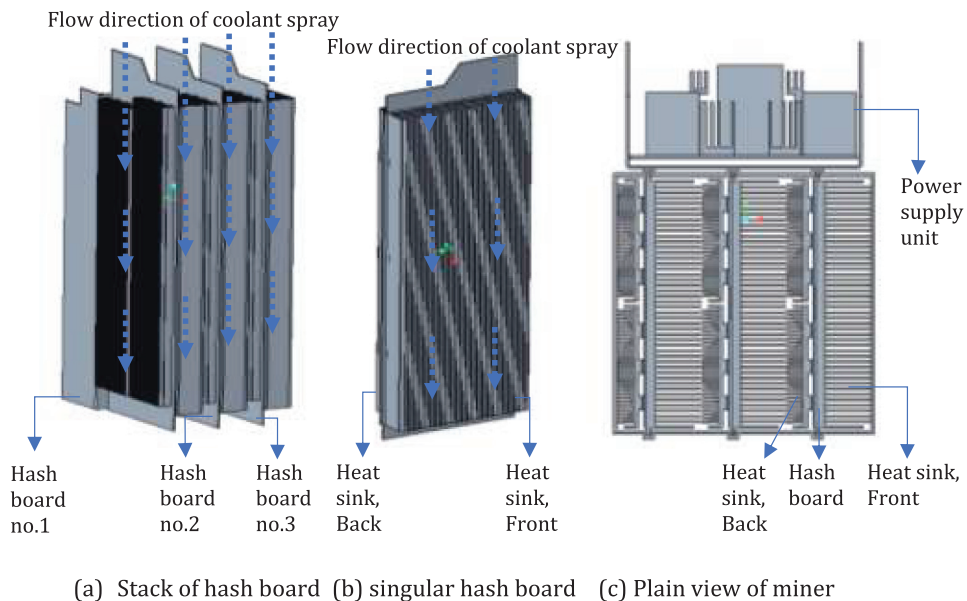


**Figure 2.** Schematic diagram of coolant spraying design. (a) Stack of hash board, (b) singular hash board, and (c) plain view of miner.



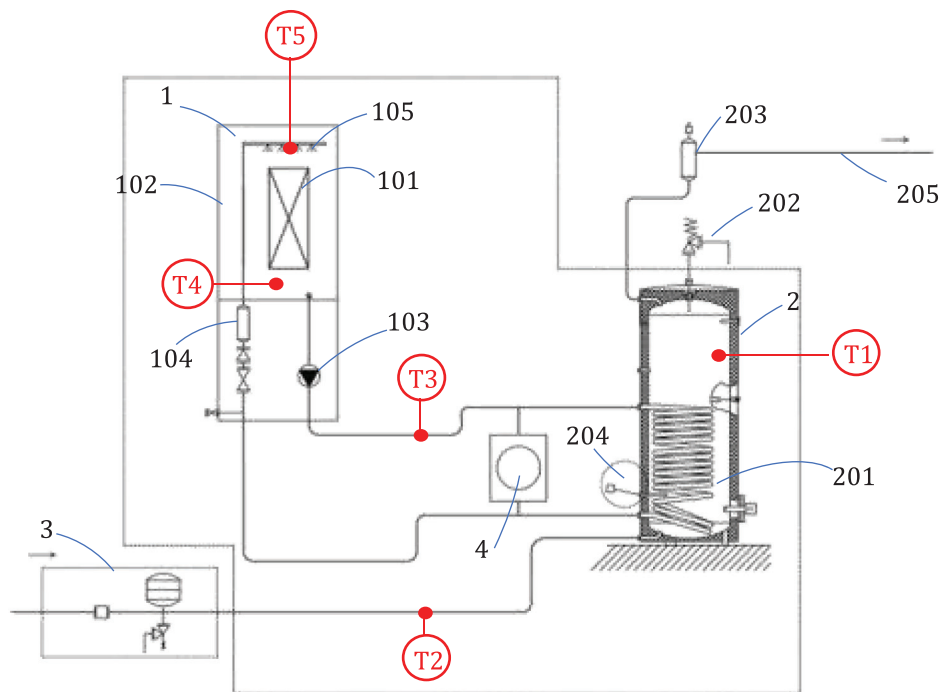


**Figure 3.**  
 Typical configurations of a digital boiler. 1 mining liquid cooling chassis, 101 miner, 102 enclosure, 103 pump, 104 Filter, 105 sprayer, 2 water tank kit, 201 Spiral coil, 202 relief valve, 203 air purger, 204 liquid level controller, 205 supply water line, 3 water replenishing kit, 4 dry cooler.

spiral coil in the water tank (a 190 L insulated tank). The internal volume of the water tank would be filled with fresh water from the water replenishing kit. Hot water in the water tank will be heated by coil and pushed out to the supply water line. In the supply water line, the air purger will discharge the air released from water into the ambient. The thermostat can maintain the water temperature in the water tank by controlling the bypass flow through the dry cooler partially or fully in response to the load requests. Thermocouples connected with the datalogger have been put at the positions shown in **Figure 3** for testing purposes. **Figure 4** indicates the main components and their installation of a prototype. **Figure 5** is the image of a real digital boiler, which has the exact compatible geometrical size and connections with the current electric/gas water heater. **Table 1** shows the main parameters of Digital Boiler.

#### 4. Performance of digital boiler

As a key parameter of heat recovery, the max. Water temperature has been studied under the steady, reliable, and continuous operation of miners. **Figure 6** presents the variation of power, average temperature of hash boards and frequency of hash board with different spraying coolant temperature. It can be found in **Figure 6** that under a certain spraying flowrate, the miner power consumption, hash rate, and frequency have a very limited rising with the increase of dielectric coolant temperature (T4 in **Figure 3**). It implies that the miner can deliver a constant hashing rate in parallel with

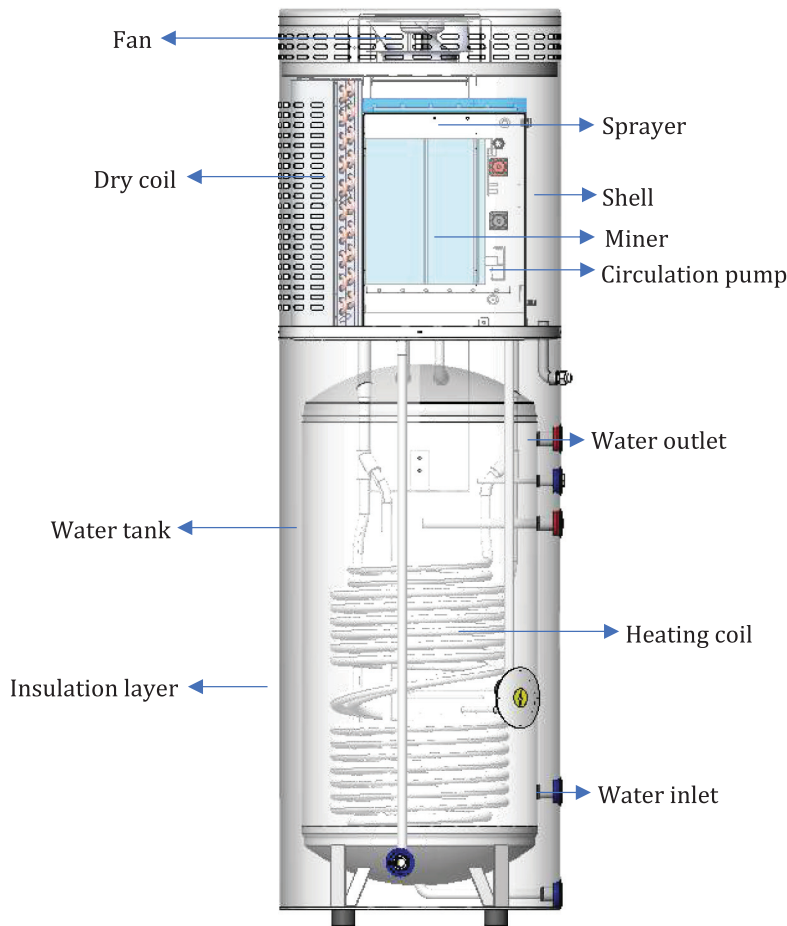
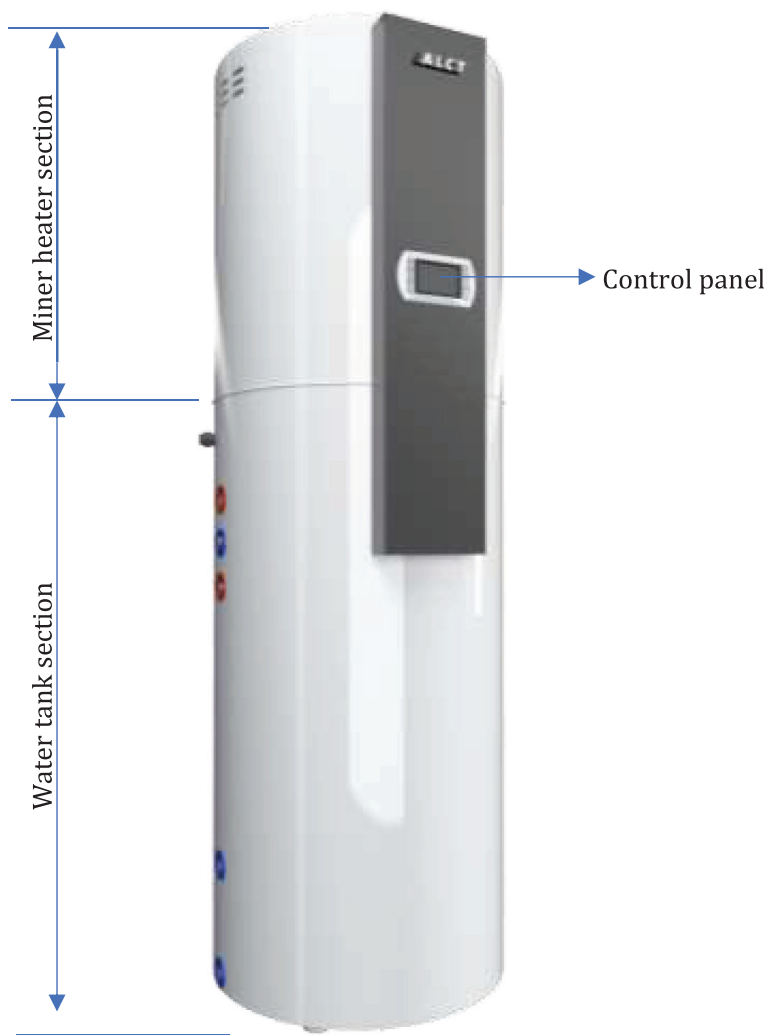


**Figure 4.**  
*Drawing of digital boiler.*

stable thermal output. The average temperature of hash boards read from Whatsminer-M3x&M5x firmware has a linear trend with the dielectric coolant temperature. At the 45°C spraying dielectric coolant temperature ( $T_5$  in **Figure 3**), the temperature differential between the hash board and dielectric coolant is 10.17°C; At the max. Spraying dielectric coolant temperature of 65°C, the temperature differential between the hash board and the coolant is 8.50°C. Lower temperature differential at higher dielectric coolant temperature can be attributed to the viscosity reduction under higher spraying dielectric coolant temperature, which is a positive factor to elevate the dielectric coolant temperature further. To avoid triggering the auto frequency throttling mechanism for internal temperature protection [29], spraying coolant temperature is set as 65°C with safety tolerance for this miner without sacrificing its reliability.

**Figure 7** reveals the trend of spray coolant temperature ( $T_5$  in **Figure 3**) and hash board temperature as the function of coolant flowrate. The temperature differential between spraying coolant and hash board will reduce with the increase of coolant



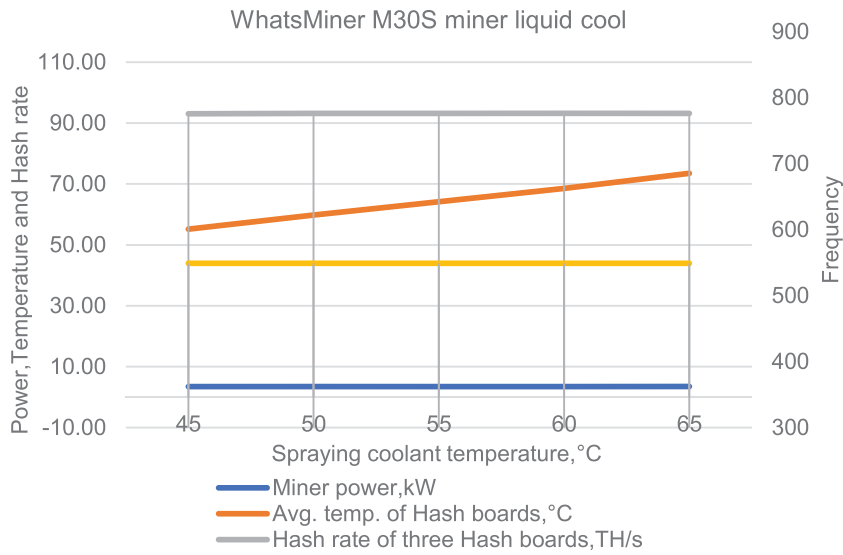


**Figure 5.**  
*Real image, and sections of digital boiler.*

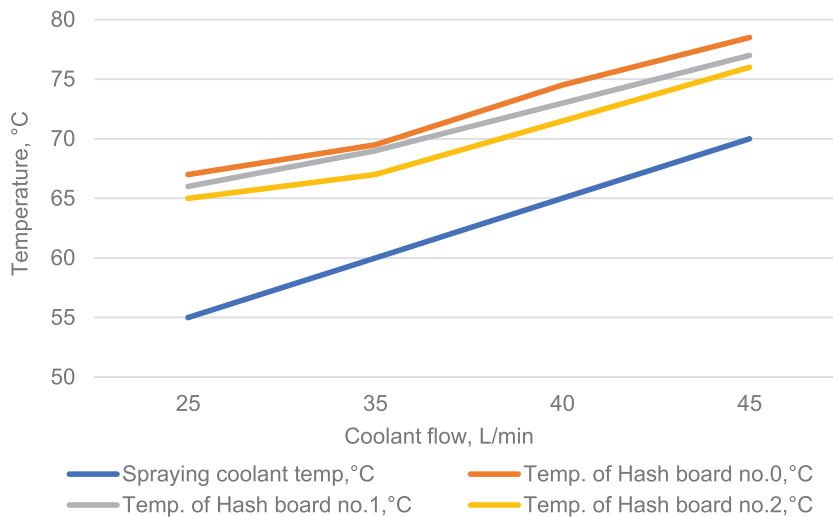
Height (mm)	Diameter (mm)	Weight (kg)	Nominal volume (L)	Water inlet/ out (inch)	Insulation layer (mm)	Electrical energy input (kW)
1950	600	114	190	¾ NPT	50.8	3.4

**Table 1.**  
*Digital boil performance as a residential water heater.*

flow. For example, the temperature differential between spraying coolant and the hash board no.2 is 10°C at the flow rate of 25 L/min and decreased to 6°C at the flow rate of 45 L/min. It can be attributed to the compound effects of viscosity reduction under higher temperatures and the flush velocity increase with more coolant. This trend implies a possible approach to elevate the coolant temperature further. In addition, it can be found that with the increased coolant flow to 45 L/min, max. 70°C

**Figure 6.**

Variation of power, average temperature of hash boards and frequency of hash board with different spraying coolant temperature.

**Figure 7.**

Variation of hash boards' temperature with different spraying coolant flow rate.

coolant temperature can be achieved with a hash board temperature under 80°C due to the minimized temperature differential by enhanced spraying momentum. This high coolant temperature can not only provide high exergy output for high-grade heat recovery but also provide the capability to kill the legionella in the water system within minutes. To minimize the legionellosis risk for building water systems has been defined compulsorily by ASHARE and CDC as a national code [30–33]. Reviewing the maximum temperature achieved in previously published single-phase dielectric liquid cooling solutions [7–9, 34, 35], 50°C can be considered a record that cannot meet the primary safety requirements of a building water system.

Reviewing the evolution of district energy technologies [36], the operation temperature categorized by International Renewable Energy Agency is dropping from approx. 200°C of First-generation district heating which was based on the steam system, and transferred by steam pipes in concreted ducts during Y1880–Y1930, to the range of 50–70°C of Fourth generation district heating which is based on the smart energy during Y2020–Y2050, including an optimum interaction system of sustainable energy sources, intelligent distribution system, two-way energy reservoir, and end consumption. From Marco and quantitative perspective, the renewable share in global district heat will be increased from 8% (30.64EJ) in Y2017 to 77% (270.27EJ) in Y2050, renewable share in electricity will be increased from 25% (95.75EJ) in Y2017 to 86%(301.86EJ) in Y2050 respectively. Refer to global trends in internet traffic, data center workloads, and data center energy use [37, 38], the global energy consumption by the data center in Y2030 will be 11.52EJ, which could provide 9.4% district heat load to Forth generation district heating directly as renewable energy, if the medium temperature reclaimed from datacenter into district heating network could catch up the range of 50–70°C. Regarding the transmission network losses, output medium temperature from the data center higher than 60°C can be considered as the bottom line to ensure the seamless integration with the Fourth general district heating network. The infrastructure of district heating can be merged with that of the data center as an integrated energy complex. From the micro perspective, the heat pump is one of the most energy-efficient and environment-friendly options to boost the low-grade thermal energy from the data center, COP of the heat pump booster under temperature lift 45°C can exceed 5.6 with some low GWP synthetic refrigerants, i.e. R1234ze and R1234zd. Their optimal working range to achieve high COP is 55–65°C evaporation temperature [39]. ORC is a thermal-electrical recovery for low-grade waste heat. The higher the water temperature is, the higher the cycle efficiency can be achieved. From either macro or micro perspectives, elevating the outlet temperature from the data center is a key to not only determining the system efficiency technically but also impacting the capital investment and revenue return economically. 60°C as the medium outlet temperature of data center heat recovery can be considered the reference temperature technically and financially.

## 5. Exergy efficiency analysis

The exergy [40] refers to the availability or quality of a thermodynamic system to a specified reference and is related to the first and second laws of thermodynamics. The availability of a thermal system is zero when in balance with the reference conditions. The physical exergy definition is given in Eq. (4) where  $h_i$  and  $h_o$  refer to the specific enthalpies and  $s_i$  and  $s_o$  refer to the specific entropies of  $i^{th}$  point and dead state conditions and  $T_0$  is the dead state or ambient temperature. The exergy factor of mechanical energy and electrical energy is 1.0 [41].

$$ex_i = h_i - h_o - T_0 \times (s_i - s_o) \quad (4)$$

The curve in **Figure 8** is the specific exergy of hot water under the condition of 1 bar pressure and variable temperature. The specific exergy at 50°C hot water (Point 1) is 4.19 kJ/kg, which is half of the specific exergy at 61°C (Point 2). It means the exergy recovered in this design is twice as much as the exergy in the current commercial liquid immersion system. The slope of this curve indicates the increasing ratio

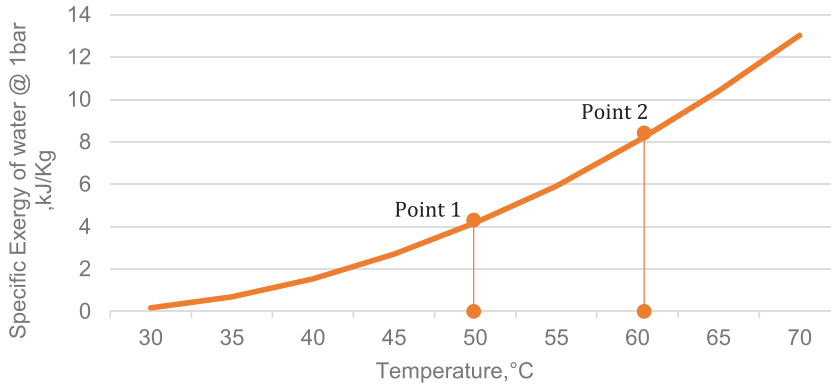


**Figure 8.**  
Exergy in hot water under different temperatures @ 1 atm.

of exergy at the higher temperature is much larger than that at the lower temperature. This characteristic reveals the essence to pursue high-grade heat recovery.

Power usage effectiveness (PUE), a concept based on the first law of thermodynamics, is a ratio that describes how efficiently a computer data center uses energy; Specifically, how much energy is used by the computing equipment in contrast to cooling and other overhead that supports the equipment, which was published in 2016 as a global standard under ISO/IEC 30134-2:2016. An ideal PUE is 1.0, given that Non-IT Facility Energy is zero, refer to Eq. (5). Anything that is not considered a computing device in a data center (e.g., lighting, cooling, etc.) falls into the category of facility energy consumption.

$$PUE_{en} = \frac{TotalFacilityEnergy}{ITEquipmentEnergy} = 1 + \frac{NonITFacilityEnergy}{ITEquipmentEnergy} \quad (5)$$

Since Total facility energy and IT equipment Energy are supplied in the form of electrical energy, the exergy factor of electrical energy is 1. Eq. (5) can be recast as follows:

$$PUE_{ex} = \frac{TotalFacilityExergy}{ITEquipmentExergy} = 1 + \frac{NonITFacilityExergy}{ITEquipmentExergy} \quad (6)$$

Regarding the exergy in the reclaimed thermal energy, the Non-IT Facility Exergy can be offset partially. The definition of  $PUE_{ex}$  in Eq. (6) involving the heat recovery will be

$$\begin{aligned} PUE_{ex} &= \frac{TotalFacilityExergy - Exergyinreclaimedheat}{ITEquipmentExergy} \\ &= 1 + \frac{NonITFacilityExergy - Exergyinreclaimedheat}{ITEquipmentExergy} \end{aligned} \quad (7)$$

The exergy efficiency of the heat reclaim system will be defined as

$$E_{re} = \frac{Exergyinreclaimedheat}{Totalfacilityexergy} \quad (8)$$

Total facility energy (kW)	IT equipment energy (kW)	$PUE_{en}$	Total facility exergy within 1 hour (kJ)	Exergy in reclaimed heat within 1 hour (kJ)	IT Equipment Exergy within 1 hour (kJ)	$PUE_{ex}$	$E_{re}$ (%)
3.40	3.30	1.03	12225.60	997.13	11880.00	0.95	8.16

**Table 2.**  
*Exergy calculation of heat reclaim.*

**Table 2** lists the testing results and derivative calculation of this prototype. The miner consumes 3.3 kW electrical energy at its nominal hash rate. The energy consumption of the circulation pump is 100 W.  $PUE$  refer to Eq. (5) would be 1.03. Total input exergy from electrical energy within 1 hour is 12225.6 kJ. Regarding the heat recovered from the miner, the specific exergy in the hot water at 63.23°C@1 atm is 9.62 kJ/kg obtained in **Figure 8**. The total reclaimed exergy at the hot water supply flow of 103.5 kg/h during its first hour of running. Based on Eqs. (6) and (8),  $PUE_{ex}$  and  $E_{re}$  will be 0.95 and 8.16% respectively. The conventional  $PUE_{en}$  is 1.03, in contrast  $PUE_{ex}$  is less than one with consideration of reclaimed exergy. As far as the rate of energy reuse is concerned,  $PUE_{ex}$  can be considered as a better index than  $PUE_{en}$  due to its characteristic energy-quality measures.

## 6. Conclusions

A water heater with the heating element as a bitcoin miner has been designed and built, in which the single-phase dielectric coolant has been sprayed on the hash boards and coupled heat sinks of the miner in steady conventional submerge. By avail of the spray momentum, the resultant heat transferring has been enhanced and validated by increased  $N_u$  in theory and up to 70°C outlet coolant temperature in the test. The temperature differential between coolant and hash board is controlled as lower as 10°C, by which the energy grade to be recovered from either centralized or decentralized mining operations has been elevated largely. From the perspective of the first law of thermodynamics, the liquid spray cooling circulation can extract the heat from miners and transfer the energy to the exterior with minimal losses. From the perspective of the second law of thermodynamics, the quality of thermal energy reclaimed in the miners, as the monotonically increasing function of the output medium temperature, has been elevated to the extent that the district heating system can be integrated seamlessly with datacentre cooling system without extra infrastructure investments, and critical hygienic codes have also been fulfilled completely.  $PUE$ , a metric used to determine the energy efficiency of a data center, has been reconsidered and redefined in the exergy flow analysis, rather than the energy flow previously. From the testing results of the prototype,  $PUE_{en}$  is 1.03 and  $PUE_{ex}$  is 0.95. The discrepancy between them tells the influence of reclaimed useful energy, which must be considered with the prevalence of energy-saving thinking in the data center industry.

This study is the initial part of the synthesis energy system integrating digital energy (energy reclaimed from extensive digital industry), fossil energy, and sustainable energy. Regarding the stable and unidirectional output characteristics of 7x24h operation in the datacentre, the reclaimed thermal energy can work as the basic component of the district heating load, which can ease the tensions in the network caused by the fluctuating sustainable energy like wind, and solar energy. With the

quickly developing electronic industry, the upper-temperature limits of chips tend to rise continuously. The electrical power generator based on ORC would be a good solution to realize the electrical-thermal-electrical close loop in the data center. The advantage of this thermal-electrical transition is the saving of access pipework to the current heating system. However, this thermal-electrical recovery is more applicable to large-scale scenarios. Considering the high start temperature of ORC, more studies are required to suit the 60–70°C heat sources.

## Abbreviations

ANSI	American National Standards Institute
ASHRAE	American Society of Heating, Refrigerating and Air-Conditioning Engineers
CDC	Centers for Disease Control and Prevention
COP	Coefficient of Performance
DC	Direct Current
GWP	Global Warming Potential
IEC	International Electrotechnical Commission
ISO	International Organization for Standardization
IT	Intelligent Technology
Nu	Nusselt number
ORC	Organic Rankine Cycle
Pr	Prandtl number
PUE	Power Usage Effectiveness
Re	Reynolds number

## Author details

Nan Chen<sup>1,2\*</sup>, Yunshui Chen<sup>2</sup> and He Zhao<sup>3</sup>


1 Advanced Liquid Cooling Technologies, Greer, USA

2 Airsys Cooling Technologies, Greer, USA

3 Airsys Singapore Pte. Ltd, Singapore

\*Address all correspondence to: [brad.chen@advancedliquidcooling.com](mailto:brad.chen@advancedliquidcooling.com)

## IntechOpen

© 2022 The Author(s). Licensee IntechOpen. This chapter is distributed under the terms of the Creative Commons Attribution License (<http://creativecommons.org/licenses/by/3.0>), which permits unrestricted use, distribution, and reproduction in any medium, provided the original work is properly cited. 



## References

- [1] Cristina C. Bitcoin consumes ‘more electricity than Argentina’ [Internet]. 2021. Available from: <https://www.bbc.com/news/technology-56012952>. [Accessed: June 24, 2022]
- [2] Gibbons L, Persoons T, Alimohammadi S. Techno-economic and sustainability analysis of potential cooling methods in Irish data Centres. *Journal of Electronics Cooling and Thermal Control*. 2021;**10**(3):35-54. DOI: 10.4236/jectc.2021.103003
- [3] Ljungqvist HM, Mattsson L, Risberg M, Vesterlund M. Data center heated greenhouses, a matter for enhanced food self-sufficiency in sub-arctic regions. *Energy*. 2021;**215**:119169. DOI: 10.1016/j.energy.2020.119169
- [4] Enachescu MS Closed Loop Cryptocurrency Mining in Alberta [Internet]. 2019. Available from: <https://prism.ucalgary.ca/bitstream/handle/1880/111108/2019%20Closed%20Loop%20Cryptocurrency%20Mining%20in%20Alberta.pdf?sequence=1&isAllowed=y>. [Accessed: June 24, 2022]
- [5] Agrodomes company website. Agrodomes: Home [Internet]. 2022. Available from: <https://agrodomes.com/>. [Accessed: June 24, 2022]
- [6] United American Corp. United Blockchain Corp Announces International Request for Proposal (RFP) For Its Proposed BlockchainDomes in Quebec for Large-scale mining operations [Internet]. 2018. Available from: <https://www.globenewswire.com/news-release/2018/01/24/1304376/0/en/United-Blockchain-Corp-Announces-International-Request-for-Proposal-RFP-For-Its-Proposed-BlockchainDomes-in-Quebec-for-Large-Scale-Mining-Operations.html>. [Accessed: June 24, 2022]
- [7] Kim MH, Ham SW, Park JS, Jeong JW. Impact of integrated hot water cooling and desiccant-assisted evaporative cooling systems on energy savings in a data center. *Energy*. 2014;**78**:384-396. DOI: 10.1016/j.energy.2014.10.023
- [8] Zimmermann S, Meijer I, Tiwari MK, Paredes S, Michel B, Poulikakos D. Aquasar: A hot water-cooled data center with direct energy reuse. *Energy*. 2012;**43**(1):237-245. DOI: 10.1016/j.energy.2012.04.037
- [9] Coles HC, Steve EG. Direct liquid cooling for electronic equipment [Internet]. 2014. Available from: [https://eta-publications.lbl.gov/sites/default/files/direct\\_liquid\\_cooling.pdf](https://eta-publications.lbl.gov/sites/default/files/direct_liquid_cooling.pdf). [Accessed: June 24, 2022]
- [10] Chi YQ, Summers J, Hopton P, Deakin K, Real A, Kapur N, et al. Case study of a data center using enclosed, immersed, direct liquid-cooled servers. In: 2014 Semiconductor Thermal Measurement and Management Symposium (SEMI-THERM). San Jose, CA USA: SEMI-THERM; 2014. pp. 164-173. DOI: 10.1109/SEMI-THERM.2014.6892234
- [11] Jesse W. North Vancouver to Be World's First City Heated by Bitcoin [Internet]. 2021. Available from: <https://www.nasdaq.com/articles/north-vancouver-to-be-worlds-first-city-heated-by-bitcoin-2021-10-14>. [Accessed: June 24, 2022]
- [12] Wisemining company website. Meet Sato [Internet]. 2022. Available from: <https://www.wisemining.io/product>. [Accessed: June 24, 2022]
- [13] Capozzoli A, Primiceri G. Cooling systems in data centers: State of art and

- emerging technologies. *Energy Procedia*. 2015;**83**:484-493. DOI: 10.1016/j.egypro.2015.12.168
- [14] Asetek, Inc. Global leader in liquid cooling Solutions [Internet]. 2022. Available from: <https://www.asetek.com/liquid-cooling/>. [Accessed: June 24, 2022]
- [15] Gaynes M, Simons R, Schmidt R, Chainer T. Server liquid cooling with chiller-less data center design to enable significant energy savings. In: 2012 28th Annual IEEE Semiconductor Thermal Measurement and Management Symposium (SEMI-THERM). San Jose, CA USA: SEMI-THERM; 2012. pp. 212-223. DOI: 10.1109/STHERM.2012.6188851
- [16] Koronen C, Åhman M, Nilsson LJ. Data centers in future European energy systems—Energy efficiency, integration, and policy. *Energy Efficiency*. 2020; **13**(1):129-144. DOI: 10.1007/s12053-019-09833-8
- [17] Marcinichen JB, Olivier JA, Thome JR. On-chip two-phase cooling of data centers: Cooling system and energy recovery evaluation. *Applied Thermal Engineering*. 2012;**41**:36-51. DOI: 10.1016/j.applthermaleng.2011.12.008
- [18] Kuncoro IW, Pambudi NA, Biddinika MK, Widiastuti I, Hijriawan M, Wibowo KM. Immersion cooling as the next technology for data center cooling: A review. *Journal of Physics: Conference Series*. 2019; **1402**(4):044057. DOI: 10.1088/1742-6596/1402/4/044057
- [19] Finch A. Mechanics of Spray Cool Direct Spray [Internet]. 2009. Available from: [https://www.parker.com/literature/Gas%20Turbine%20Fuel%20Systems%20Division/TMS%20Microsite%20Literature%20files/PH\\_WP\\_Mechanics\\_of\\_SprayCool\\_direct\\_spray.pdf](https://www.parker.com/literature/Gas%20Turbine%20Fuel%20Systems%20Division/TMS%20Microsite%20Literature%20files/PH_WP_Mechanics_of_SprayCool_direct_spray.pdf). [Accessed: June 24, 2022]
- [20] Gao X, Li R. Spray impingement cooling: The state of the art. In: *Advanced Cooling Technologies and Applications*. Vol. 5. London: IntechOpen; 2018. pp. 27-51. DOI: 10.5772/intechopen.80256
- [21] Soriano GE, Zhang TL, Alvarado JL. Study of the effects of single and multiple periodic droplet impingements on liquid film heat transfer. *International Journal of Heat and Mass Transfer*. 2014; **77**:449-463. DOI: 10.1016/j.ijheatmasstransfer.2014.04.075
- [22] Zhang TL, Alvarado JL, Muthusamy JP, Kanjirakat A, Sadr R. Numerical and experimental investigations of crown propagation dynamics induced by droplet train impingement. *International Journal of Heat and Fluid Flow*. 2016;**57**:24-33. DOI: 10.1016/j.ijheatfluidflow.2015.10.003
- [23] Zhang TL, Alvarado JL, Muthusamy JP, Kanjirakat A, Sadr R. Heat transfer characteristics of double, triple and hexagonally-arranged droplet train impingement arrays. *International Journal of Heat and Mass Transfer*. 2017; **110**:562-575. DOI: 10.1016/j.ijheatmasstransfer.2017.03.009
- [24] Gao X, Li R. Impact of a drop burst flow on a film flow cooling a hot surface. *International Journal of Heat and Mass Transfer*. 2018;**126**:1193-1205. DOI: 10.1016/j.ijheatmasstransfer.2018.06.042
- [25] Chen H, Cheng WL, Peng YH, Zhang WW, Jiang LJ. Experimental study on optimal spray parameters of piezoelectric atomizer-based spray cooling. *International Journal of Heat*

- and Mass Transfer. 2016;**103**:57-65.  
DOI: 10.1016/j.ijheatmasstransfer.2016.07.037
- [26] Rybicki JR, Mudawar I. Single-phase and two-phase cooling characteristics of upwardfacing and downward-facing sprays. *International Journal of Heat and Mass Transfer*. 2006;**49**:5-16.  
DOI: 10.1016/j.ijheatmasstransfer.2005.07.040
- [27] Holman JP. *Heat Transfer*. 7th ed. Southern Methodist University, McGraw Hill Book Company; 1989. p. 736
- [28] Delgado San Román F, Fernández Diego I, Urquiza Cuadros D, Mumyakmaz B, Unsal A. Fluid-thermal analysis of the cooling capacity of a commercial natural ester in a power transformer. *Renewable Energy and Power Quality Journal (RE&PQJ)*. 2013; **1**(11):1158-1163. DOI: 10.24084/repqj11.564
- [29] Shenzhen MicroBT Electronics Technology Co., Ltd. *Whatsminer M30S Manual* [Internet]. 2019. Available from: <https://www.zeusbtc.com/manuals/user-manuals/WhatsMiner-M30S-Manual.pdf>. [Accessed: June 24, 2022]
- [30] ASHRAE. *ANSI/ASHRAE Standard 188-2018. Legionellosis: Risk management for building water systems establishes minimum legionellosis risk management requirements for building water systems*. 2018
- [31] ASHRAE Guideline 12-2000. *Minimizing the Risk of Legionellosis Associated with Building Water Systems*
- [32] U.S. Department of Health and Human Services Centers for Disease Control and Prevention (CDC). *Guidelines for environmental infection control in health-care facilities* [Internet]. 2003. Available from: Guide lines for environmental infection control in health-care facilities (cdc.gov). [Accessed: June 24, 2022]
- [33] U.S. Department of Energy. *Water heater test procedure rulemaking: development testing preliminary report* [Internet]. 2013. Available from: [https://www1.eere.energy.gov/buildings/appliance\\_standards/pdfs/water\\_heater\\_test\\_report\\_111413.pdf](https://www1.eere.energy.gov/buildings/appliance_standards/pdfs/water_heater_test_report_111413.pdf). [Accessed: June 24, 2022]
- [34] GRC. *Powerful immersion cooling technology in an incredibly compact, plug-n-play package* [Internet]. 2021. Available from: [https://www.grcooling.com/wp-content/uploads/2021/03/grc\\_data\\_sheet\\_iceraq\\_micro.pdf](https://www.grcooling.com/wp-content/uploads/2021/03/grc_data_sheet_iceraq_micro.pdf). [Accessed: July 5, 2022]
- [35] Submer. *Micropod technical specs* [Internet]. 2022. Available from: <https://submer.com/micropod/>. [Accessed: July 5, 2022]
- [36] Federal Ministry for the Environment, Nature Conservation and Nuclear Safety. *Integrating low-temperature renewables in district energy systems: Guidelines for policy makers* [Internet]. 2021. Available from: [https://irena.org/-/media/Files/IRENA/Agency/Publication/2021/March/IRENA\\_District\\_Energy\\_Systems\\_2021.pdf](https://irena.org/-/media/Files/IRENA/Agency/Publication/2021/March/IRENA_District_Energy_Systems_2021.pdf). [Accessed: July 30, 2022]
- [37] Benjamin KS, Chukwuka GM, Paul U. Making the internet globally sustainable: Technical and policy options for improved energy management, governance and community acceptance of Nordic datacenters. *Renewable and Sustainable Energy Reviews*. 2022;**154**: 1-20. DOI: 10.1016/j.rser.2021.111793
- [38] Liu Y, Wei X, Xiao J, Liu Z, Xu Y, Tian Y. Energy consumption and emission mitigation prediction based on data center traffic and PUE for global data centers. *Global Energy*

Interconnection. 2020;3:272-282.  
DOI: 10.1016/j.gloei.2020.07.008

[39] Wang RZ, Xu ZY, Hu B, Du S, Jiang L, Wang LW. Heat pumps for efficient low grade heat uses: From concept to application. *Thermal Science and Engineering*. 2019;27:1-15.  
DOI: 10.11368/tse.27.1

[40] Trusler JPM. T-S diagram for water [Internet]. 2003. Available from: <https://www.imperial.ac.uk/media/imperial-college/research-centres-and-groups/thermophysics/Chart-T-s-Water.pdf>. [Accessed: June 24, 2022]

[41] Gong M, Wall G. Exergy analysis of the supply of energy and material resources in the Swedish society. *Energies*. 2016;9(9):707. DOI: 10.3390/en9090707